

Temperature dependence of the electromechanical properties of 0-3 PbTiO₃-polymer piezoelectric composite materials

Kurt M. Rittenmyer

Naval Research Laboratory, Underwater Sound Reference Detachment, P.O. Box 568337, Orlando, Florida 32856-8337

(Received 24 September 1993; accepted for publication 16 March 1994)

The electromechanical properties of 0-3 ceramic-polymer composite piezoelectric materials manufactured by NTK Corporation in Japan have been measured as a function of temperature using several techniques. The elastic, dielectric, and piezoelectric constants were measured by fitting the complex admittance vs frequency spectrum to a model of a piezoelectric resonator near the electromechanical resonance [Xu *et al.*, *J. Wave Mater. Interact.* **2**, 105-181 (1987)]. These properties are shown to vary significantly with temperature as a result of the glass-transition region of the polymer phase. The theory of viscoelasticity in polymers discussed by Ferry (WLF theory), which explains the influence of the glass transition on the elastic properties of polymers, is used to describe the temperature dependence of the elastic and dielectric properties of the composite materials. The temperature dependence of the dielectric permittivity is shown to be similar in form to the temperature dependence of the elastic properties. For a material with larger filler particles, the temperature dependence corresponds exactly. For materials containing smaller particles, the magnitude of the time-temperature superposition shift parameters are not consistent for the different properties. The application of the time-temperature superposition principle for shifting experimental data to account for differences in measurement frequencies and temperatures is demonstrated. These measurements are compared with independent elastic property measurements and with results from thermal analysis. They are found to be consistent. Values for Poisson's ratio are calculated using independent measurements of the elastic constants S_{11}^E and C_{33}^D . The observed properties can be related to the structure of the composite material.

PACS numbers: 43.38.Ar, 43.38.Fx, 43.30.Yj

INTRODUCTION

A method for measuring electromechanical properties of mechanically lossy materials was described by Xu *et al.*¹ Since many new piezoelectric composite materials intended for transduction applications consist of a piezoelectric ceramic embedded in a polymer material, the behavior of their elastic properties is, in many respects, similar to that of conventional carbon-loaded polymers. This is particularly true of the NTK piezoelectric composite materials which are composite materials consisting of lead titanate particles embedded in a polychloroprene rubber. They are manufactured by NTK Corporation which is a subsidiary of NGK Spark Plug Company Ltd of Japan. The diameter of the particles of ceramic in NTK 305™ (Trademark of NTK Corp.) are approximately five times the diameter of the particles in NTK 306™ (Trademark of NTK Corp.), which are on the order of 3-4 μm. The materials differ in color and hence, the polymer phases are undoubtedly different.

The temperature dependence of the elastic properties of polymers is largely determined by the location and extent of the glass-transition region of the polymer phase, as described in numerous texts on viscoelasticity.²⁻⁵ The elastic properties, in turn, influence the transduction characteristics of the material; it is, therefore, important to quantify the elastic, dielectric, and piezoelectric properties of these materials in order to systematize design procedures for transduction applications.

The following article describes measurements of the temperature dependence of the elastic, dielectric, and piezo-

electric properties of the NTK 0-3 composite materials. The "0-3" designates the dimensionality of each phase. The "0" implies that the ceramic phase is connected in no dimension while the "3" indicates connectedness in 3 dimensions for the polymer phase. These results are compared with measurements of the thermal properties using differential scanning calorimetry and with two independent measurements of elastic stiffness.

I. VISCOELASTIC THEORY

A. Definitions of complex elastic constant functions

The theory of viscoelasticity in homogeneous polymeric and filled polymeric materials is described in detail in numerous textbooks and articles.²⁻⁵ Most unoriented polymers, including the ones considered here, are isotropic and their elastic properties are described by complex functions of frequency. For discussion purposes only, we assume the NTK materials are elastically isotropic. This assumption will not be applied except for rough estimation. A description of the actual parameters measured is given in the next section. For dielectric and elastic properties, this assumption is not unreasonable since, unlike polyvinylidene fluoride (PVDF), the material is isotropic prior to poling. If the electromechanical coupling is fairly low, the anisotropy in the dielectric and elastic properties will only be on the order of a few percent. The complex shear modulus may be written in the form,

$$G^*(\omega) = G'(\omega) + iG''(\omega) = G'(1 + i \tan \delta_{mG}), \quad (1)$$

while the complex bulk modulus is expressed as,

94-24744

1328

94 8 04 042

$$K^*(\omega) = K'(\omega) + iK''(\omega) = K'(1 + i \tan \delta_{mK}), \quad (2)$$

The superscript asterisk indicates a complex-valued property consisting of a real part, labeled as single-primed characters, which relates the strain in phase with the applied harmonic stress to the applied stress itself, and the double-primed quantities, which represent the ratio of strain that is out of phase with applied stress to the applied stress. $\tan \delta_{mG}$ and $\tan \delta_{mK}$ are the loss tangents associated with shear modulus and bulk modulus, respectively. For isotropic materials, the elasticity tensor is fully described by two independent elastic moduli. The shear and bulk moduli are commonly used together. Other elasticity functions of interest which can be expressed in terms of $G(\omega)$ and $K(\omega)$ include Young's modulus,

$$E^*(\omega) = E'(\omega) + iE''(\omega) = \frac{9K^*(\omega)G^*(\omega)}{G^*(\omega) + 3K^*(\omega)}, \quad (3)$$

and the bulk longitudinal or plane-wave modulus,

$$M^*(\omega) = M'(\omega) + iM''(\omega) = K^*(\omega) + (4/3)G^*(\omega). \quad (4)$$

If two of the elasticity functions are known, the other two can be calculated using Eqs. (3) and (4). The shear modulus and Young's modulus are related by

$$E^*(\omega) = 2(1 + \nu)G^*(\omega). \quad (5)$$

If the temperature of the polymer is in the rubbery region, Poisson's ratio ν virtually equals 0.5, so to close approximation,

$$E^*(\omega) = 3G^*(\omega), \quad (6)$$

and one measurement of either E or G in addition to one measurement of either K or M will determine all four elastic moduli at one particular frequency.

In the analysis that follows, the thickness modes of thin circular plates and transverse length-extensional modes of thin bars of two piezoelectric composite materials are examined at temperatures in the rubbery, glass, and transition regions. The elastic properties of the composite materials discussed here are nearly isotropic and determined, to a large extent, by the elastomer phase. Therefore, in the rubbery region of the polymer, the value of the bulk modulus $K(\omega)$ and the plane-wave modulus $M(\omega)$ of the composite material are nearly equal to c_{33}^D and relate directly to measurements of the fundamental thickness resonance. The bulk longitudinal wave speed associated with the thickness drive is given by

$$\nu_b = (c_{33}^D/\rho)^{1/2} \doteq [M'(\omega)/\rho]^{1/2}. \quad (7)$$

For materials that are nearly elastically isotropic, the value of Young's Modulus $E(\omega)$ is virtually equal to the reciprocal of the elastic compliance, $(S_{11}^E)^{-1}$, and is directly related to the extensional wave speed in a thin rod by

$$\nu_1(\omega) = [\rho S_{11}^E(\omega)]^{-1/2} \doteq [E(\omega)/\rho]^{1/2}, \quad (8)$$

where ρ is the density of the material. If any sample dimension is close to a wavelength (i.e., if the sample is not "thin"), then the plane-wave modulus is appropriate since it accounts for the lateral clamping of the extensional mode that is present under such conditions. The elastic properties

of the NTK 0-3 composites are only slightly anisotropic and the approximate relationships defined in Eqs. (7) and (8) are not unreasonable. However, for a highly anisotropic composite material, such as one constructed from rods or fibers aligned in a single direction, the shear modulus and plane-wave modulus will vary significantly depending on the direction of the applied stress. The appropriate tensor formalism is required for such materials.⁶

The relaxation mechanisms in polymers are not generally simple but usually can be modeled by assuming the relaxation times to be statistically distributed in some fashion. For the shear modulus, the statistical distribution is described by the relaxation spectrum $H(\tau)$ which is related to the real and imaginary components of the shear modulus by the integral equations,

$$G'(\omega) = \int_0^\infty \frac{\omega^2 \tau^2}{(1 + \omega^2 \tau^2)} H(\tau) d(\log \tau) \quad (9)$$

and

$$G''(\omega) = \int_0^\infty \frac{\omega \tau}{(1 + \omega^2 \tau^2)} H(\tau) d(\log \tau). \quad (10)$$

Information about the relaxation spectrum, which is often assumed to be a Gaussian distribution, can be obtained by a variety of measurements including those of the viscoelastic properties. Expressions such as Eqs. (9) and (10) for the other elastic moduli are given in the texts by Ferry² and Bailey *et al.*³

B. Effect of glass transition on mechanical properties

The glass transition in polymers can be studied by examining resonance-relaxation phenomena in the elastic and dielectric properties that are associated with this second-order phase transition. At low temperature, the polymer is glasslike with high elastic moduli and low mechanical losses. As the temperature is increased into the transition zone, the real part of the elastic moduli will decrease and the mechanical loss will increase before reaching a peak which defines the actual glass-transition temperature T_g . The mechanical loss then decreases somewhat as temperature increases into the rubbery region. For highly damped materials, the loss will decrease only moderately as the temperature is raised, and the transition in the real part of the modulus appears at a lower temperature relative to the peak in the loss modulus. For materials with low damping, the loss modulus decreases back toward the values at low temperatures and the peak in the loss occurs very near the temperature at which the relaxation in the elastic modulus is centered.

The behavior of the dielectric properties of some polymers often mirror the behavior of the elastic properties over certain regions of the frequency spectrum.²⁻³ This occurs when the motion of the main chain segments of the polymer control both dielectric and elastic properties. In this case, the shift function, $a_T(T)$, can be determined from either dielectric or elastic constant measurements. However, this may not be true over wide regions of frequency, especially for more complex and highly reinforced polymers. Motion of the side chains and interfacial effects often dominate the dielectric

properties in this case. This assumption may be even less valid for the highly polar particles of ferroelectric ceramic filler contained in the composite materials considered here. For this reason, the shift factor determined from dielectric data is denoted as $b_T(T)$. If the functional forms of the shift factors are the same, $b_T(T)$ can be substituted for $a_T(T)$ in the equations discussed below, although the coefficients in the equations may vary between dielectric and elastic measurements.

Above the glass-transition temperature, the elastic properties of many polymers vary with relaxation time τ and consequently with frequency ω in the manner described by the Williams-Landel-Ferry (WLF) equation.²

$$\log a_T(T) = \ln \left(\frac{\omega \tau}{\omega_0 \tau_0} \right) = \frac{-c_1^0(T - T_0)}{c_2^0 + T - T_0} \quad (11)$$

The shift factor a_T describes the shift in the relaxation time induced by a change in temperature. The empirically determined constants c_1^0 and c_2^0 are material parameters but do not vary widely over particular classes of polymers. Here, T_0 is the dilatometric (nonequilibrium) transition temperature. The function $a_T(T)$ can be determined by matching measurements made over a fixed range of frequencies at numerous different temperatures. The value of T_0 can be determined by fitting experimental data to Eq. (11) but it may be initially approximated by assuming it is 50 °C above T_g according to Ferry.² Examination of Eqs. (9) through (11) shows that the characteristic relaxation times τ_i only occur as products with the frequency ω . The relationship between relaxation time, frequency, and temperature is therefore defined by Eqs. (9) through (11) for temperatures above T_g . Above the glass-transition temperature, the difference in the thermal expansion of the material between the glassy state and the rubbery state results from free volume created in the structure due to thermal motion. This free volume is responsible for the observed relaxation in the electromechanical properties. An additional contribution to the free volume, and consequently to the relaxation time, results from the nonequilibrium contributions caused by the finite time required in either dynamic-mechanical or thermal measurements. This Arrhenius-like contribution, important below T_g , can be included in the right-hand side of Eq. (11). Corrections which generalize the WLF equation to cover a range of temperature below T_g have been described by Rusch and Beck.⁷ This is a special case of many other relaxation mechanisms that generally follow an Arrhenius-type dependence on temperature. The constant A_T is sometimes interpreted as an energy that is required to overcome attractive forces and activate a "hopping" motion which ultimately relaxes as the frequency of the thermal motion increases. This interpretation is often too simple, although for many cases the equation is experimentally valid. The shift factor is described by

$$\log a_T = \frac{A_T}{k} \left(\frac{1}{T} - \frac{1}{T_r} \right), \quad (12)$$

where k is Boltzman's constant, T_r is the reference temperature, and a_T is the elastic shift factor. Again, A_T may or may not be the same for dielectric and elastic properties.

C. Effect of filler materials on the elastic properties of polymers

Composite materials such as NTK 305 and NTK 306 are actually filled polymers where the filling material PbTiO_3 is ferroelectric. For NTK 306, the diameter of the filler particles is of the order of 3–4 μm which is approximately a factor of five smaller than that of NTK 305. The influence of adding filler materials on the elastic properties of polymers has been previously studied.^{2-4,8}

II. EXPERIMENTAL PROCEDURE

A. Summary of measured properties

The thermodynamic glass transition temperatures T_g of both NTK 305 and NTK 306 were determined from measurements of the enthalpy of transition using a Perkin-Elmer model DSC-4 differential scanning calorimeter and scanning from -60 °C to +20 °C. The electromechanical properties of the two composite materials produced by NTK Corporation in Japan were measured using the resonance technique described in Ref. 1. Measurements were performed over the temperature range from -70 °C to +50 °C at increments of ten degrees except near the glass-transition temperature region where the increment was reduced to five degrees in order to define the transition more precisely. The method is applicable to both thickness (TE) modes of vibration as well as transverse length extensional (LT) modes. The measured parameters for the thickness drive include the electromechanical coupling factor k_1 , the elastic stiffness c_{33}^D , and the clamped dielectric permittivity, ϵ_{33}^S , and their associated loss tangents, $\tan \delta_{k_1}^D$, $\tan^D \delta_m$ and $\tan^S \delta_e$, respectively. For the length extensional drive, the transverse electromechanical coupling factor k_{31} , the open-circuit compliance S_{11}^E , and the free dielectric constant ϵ_{33}^T , and each of their associated loss tangents are determined. Since all of the parameters are treated as complex, a loss tangent is associated with each parameter as given in the following equations:

$$c_{33}^D = c_{33}^D (1 + i \tan^D \delta_m), \quad (13)$$

$$S_{11}^E = S_{11}^E (1 - i \tan^E \delta_m), \quad (14)$$

$$\epsilon_{33}^S = \epsilon_{33}^S (1 - i \tan^S \delta_e), \quad (15)$$

$$\epsilon_{33}^T = \epsilon_{33}^T (1 - i \tan^T \delta_e), \quad (16)$$

$$k_1^2 = k_1^2 (1 + i \tan \delta_{k_1}^2), \quad (17)$$

and

$$k_{31}^2 = k_{31}^2 (1 + i \tan \delta_{k_{31}}^2). \quad (18)$$

Therefore, there are 12 parameters defined in Eqs. (13)–(18) that are determined by the resonance technique for each material. While this does not represent the entire set of elastic, piezoelectric, and dielectric tensor components, it does include those that are pertinent to most transducer applications and can be measured by the method of Xu *et al.*¹ The signs in the equations above result from defining the time dependence of the energy loss of the applied stress as $e^{-i\omega t}$. This ensures that a positive loss modulus is associated with en-

ergy dissipation in either the elastic or electric case. Therefore, loss tangents associated with elastic and dielectric stiffnesses, the inverse of dielectric permittivity, are positive, and loss tangents associated with the elastic compliances and dielectric permittivities are always negative.

The property coefficients described in Eqs. (13)–(18) are calculated directly from the measured values of complex admittance near the fundamental resonances. From these coefficients, the complex piezoelectric coefficients can be calculated using the formulas,

$$e_{33}^2 = k_7^2 c_{33}^D \epsilon_{33}^S, \quad (19)$$

$$h_{33}^2 = k_7^2 (c_{33}^D / \epsilon_{33}^S), \quad (20)$$

$$d_{31}^2 = k_{31}^2 s_{11}^L \epsilon_{33}^L, \quad (21)$$

and

$$g_{31}^2 = k_{31}^2 (s_{11}^L / \epsilon_{33}^L), \quad (22)$$

where Eqs. (19) and (20) apply to the thickness resonance and Eqs. (21) and (22) apply to the length extensional resonance.

An independent measurement of the elastic properties provides a check on the resonance results. In addition, if performed at different temperatures, this measurement yields a frequency-independent baseline to which measurements at various frequencies can be referred. The principle of time-temperature superposition can then be applied to correlate different elastic constant measurements at various frequencies if the shift parameter a_T is known.

By applying this technique to the composite material measurements, a value for the real part of Poisson's ratio ν , defined for a nearly isotropic material as

$$\nu^f = \nu_{12}^f = \frac{-s_{12}^f}{s_{11}^f} \doteq \nu_{13}^f = \frac{-s_{13}^f}{s_{11}^f}, \quad (23)$$

can be estimated from measurements of c_{33}^D and s_{11}^L made at identical frequencies. The value of Poisson's ratio for contraction along the polar axis is assumed to be equal to Poisson's ratio for contraction along a nonpolar direction. The two elastic constants are related approximately by the equation,

$$c_{33}^E = \frac{1 - \nu^f}{1 - \nu^f - 2(\nu^f)^2} (s_{11}^f)^{-1}, \quad (24)$$

The time-temperature superposition principle can be used to shift the c_{33}^D versus temperature curve to account for any difference in the measurement frequency between it and s_{11}^L using the appropriate shift factor. The short-circuit stiffness c_{33}^E is calculated from the open-circuit value, c_{33}^D , using the thickness coupling factor k_7 , in the formula,

$$c_{33}^E = c_{33}^D (1 - k_7^2) \quad (25)$$

to account for the difference in boundary conditions. A value for Poisson's ratio can then be calculated using the product of the experimental values of c_{33}^D and s_{11}^L and applying Eq. (25) followed by Eq. (24) and solving either directly or iteratively for the complex value of ν^f .

B. Experimental procedure for determining electromechanical properties

The following procedure was used to evaluate the electromechanical properties of mechanically lossy piezoelectric materials. The temperature of the sample was stabilized in a computer-controlled oven with liquid nitrogen cooling. The sample was cooled initially to -60°C and was then heated in 10-deg increments to $+50^\circ\text{C}$. In order to detect when thermal equilibrium had been obtained, the temperature of the sample chamber was monitored with a thermistor. The measurements of capacitance and conductance were made over a frequency range from 1–200 kHz. Peaks in the dielectric loss tangent frequently appear near 0°C in dielectric measurements due to the presence of water in the sample. Samples were kept in a desiccator prior to measurements and were heated before the run to eliminate any moisture. The experimental data were recorded and the sample was heated to the next temperature of interest. The electromechanical parameters were then extracted from the measured data using the resonance method of Xu *et al.*¹ In order to extrapolate the measured parameters for the calculation of Poisson's ratio using Eq. (25), the appropriate shift factor, as defined in either Eqs. (11) or (12), must be determined so that the values of s_{11}^L and c_{33}^D are known at the same frequency and temperature.

C. Independent measurements of elastic properties

Measurements of $(s_{11}^L)^{-1}$ were also performed using a vibrational resonance technique and then applying the WLF techniques to extend the measurement frequency over several decades. The technique is outlined briefly here. More detail is given by Ferry² and Capps.⁹ For these measurements, narrow bars with nearly square cross section of 5 to 10 mm² and lengths of about 13 cm were cut. The sample was attached to an electromagnetic shaker with accelerometers glued to both ends. The shaker was driven over a range of frequencies from below the first resonance (near 500 Hz) to above 7 kHz. The resonance is determined when the difference in phase between the two accelerometers is equal to 90° . The amplitude ratio and phase difference of the accelerometers along with the frequency determine both the real and imaginary parts of Young's modulus, $(s_{11}^L)^{-1}$. The equations of motion can be solved away from the resonance frequency as well if the phase and magnitude of the accelerometer response are known over a range of frequency. Thus both real and imaginary parts of $(s_{11}^L)^{-1}$ can be determined over approximately one decade of frequency. The appropriate shift factor can then be determined by matching measurements made at different temperatures which extends the measurement over several decades of frequency.^{2,9} These measurements were performed on both types of NTK material which have thin silver electrodes. Unlike the rubber electrode sometimes provided with this material, these electrodes are highly conductive and should prevent space-charge effects.

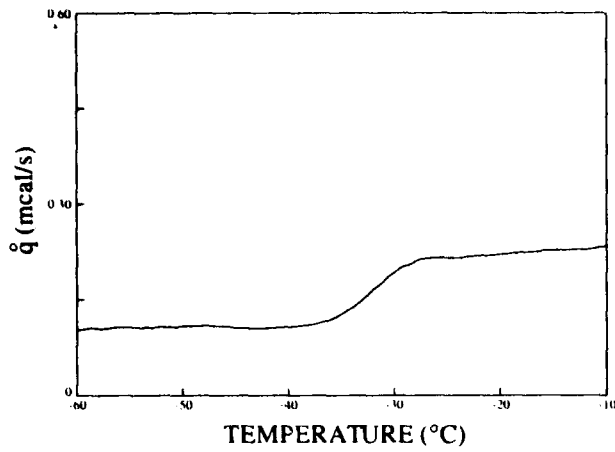


FIG. 1. Differential scanning calorimeter measurement of the rate of heat absorbed by an NTK 306 sample as a function of temperature. Heat rate was 0.67 °C/s. The glass transition appears to occur over the range -50 °C to -30 °C.

III. RESULTS

A. Differential scanning calorimeter (DSC) measurements

The results obtained by differential scanning calorimeter (DSC) clearly define the transition region for the piezorubber material. The rate of heat absorption for a sample of NTK 306 with the electrodes open-circuited and heated at a rate of 0.67 °C/s is plotted as function of temperature in Fig. 1. Figure 2 shows a similar measurement for NTK 305. The glass transition region for both materials is centered at approximately -40 °C. The results are typical of a filled polychloroprene rubber.

B. Results of measurements on NTK 305 and NTK 306 piezorubber

1. Thickness extensional (TE-33) drive parameters for NTK 306: The fundamental thickness mode series resonance frequency for the 5.1-cm-diam disk of 0.320-cm-thick NTK

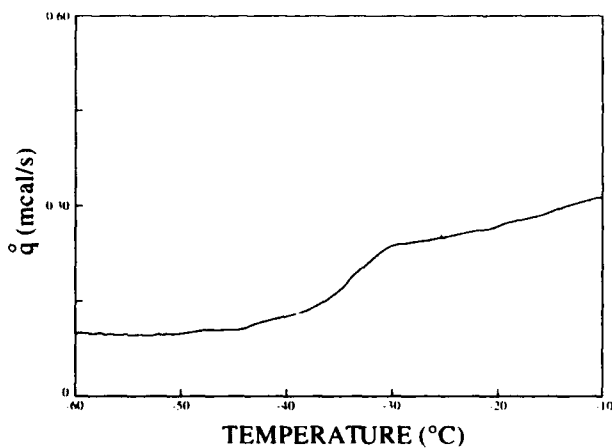


FIG. 2. Differential scanning calorimeter measurement of rate of heat absorbed by NTK 305 sample. The heating rate was 0.67 °C/s. The glass transition appears from -45 °C to -35 °C.

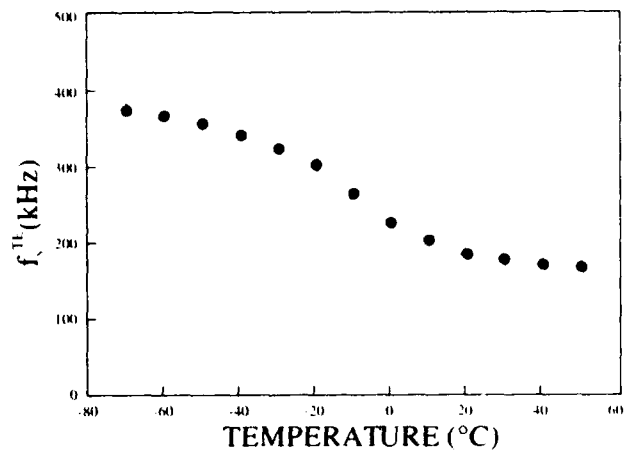


FIG. 3. Series resonance frequency, f_s^{TE} , of the fundamental thickness mode of a disk of NTK 306 piezorubber as a function of temperature.

306 material with a density of 5100 kg/m³ is plotted in Fig. 3. This curve defines the resonance frequency of the measurement of the electromechanical properties at each temperature. The relaxation in the elastic stiffness c_{33}^D is linearly related to the resonance frequency via the equation,

$$f_p^{TE} = \frac{1}{2t} \sqrt{\frac{c_{33}^D}{\rho}}, \quad (26)$$

where t is the thickness of the disk. The elastic stiffness c_{33}^D and mechanical loss tangent $\tan^D \delta_m$, are plotted as functions of temperature in Fig. 4. The real part c_{33}^D also shows a relaxation and a maximum in the mechanical loss tangent at approximately -8 °C. The temperature dependence of the clamped dielectric constant $\epsilon_{33}^D/\epsilon_0$ and of the loss tangent $\tan^D \delta$, is plotted in Fig. 5. The maximum in the loss associated with the glass transition is observed at approximately -15 °C.

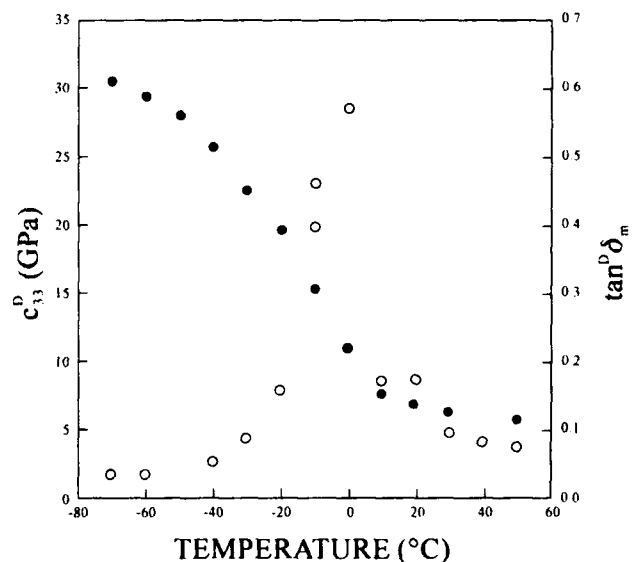


FIG. 4. Elastic stiffness, c_{33}^D (closed symbols), and the mechanical loss tangent, $\tan^D \delta_m$ (open symbols), of NTK 306 as a function of temperature. (Dashed lines are simply guides to the eye.)

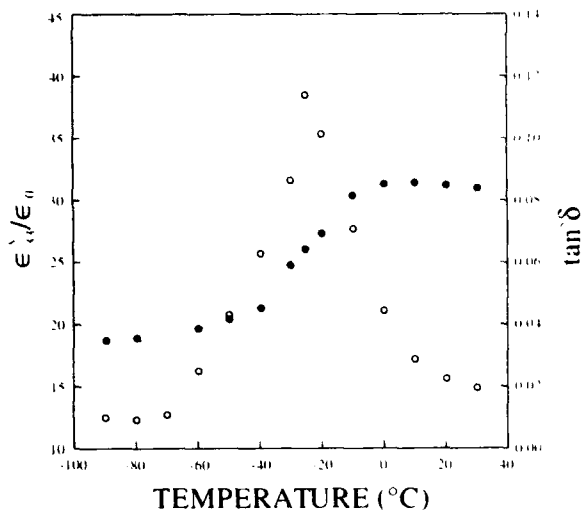


FIG. 5. Clamped dielectric constant, $(\epsilon'_{33}/\epsilon_0)$ (closed symbols), of NTK 306 and the dielectric loss tangent, $\tan \delta_k$ (open symbols), as a function of temperature.

The electromechanical coupling coefficient k_t^2 is plotted versus temperature in Fig. 6. The influence of the glass transition is again apparent. The loss tangent of the coupling factor tends to increase artificially since the model used for the calculation is not precisely representative of the physical situation. This may be caused by neglecting frequency variations in the parameters as well as sources of nonlinearity in the admittance versus frequency data. The coupling factor includes not only the losses in the piezoelectric e_{33} or h_{33} coefficient as well as the dielectric permittivity and elastic modulus, which are related by

$$k_t^2 = \frac{e_{33}^2}{c_{33}^D \epsilon_{33}^S} = \frac{h_{33}^2 \epsilon_{33}^S}{c_{33}^D} \quad (27)$$

but also contributions from these inaccurate assumptions of the model. The simple circuit model does not accurately de-

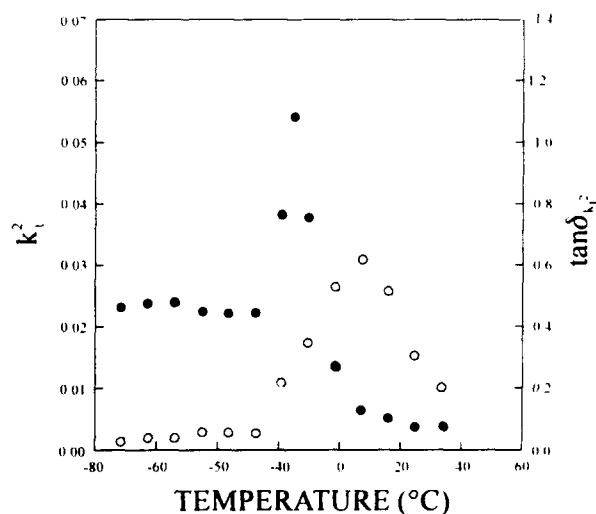


FIG. 6. Square of the thickness-extensional coupling coefficient, k_t^2 (closed symbols), and associated loss tangent, $\tan \delta_{k_t^2}$ (open symbols), of NTK 306 as a function of temperature.

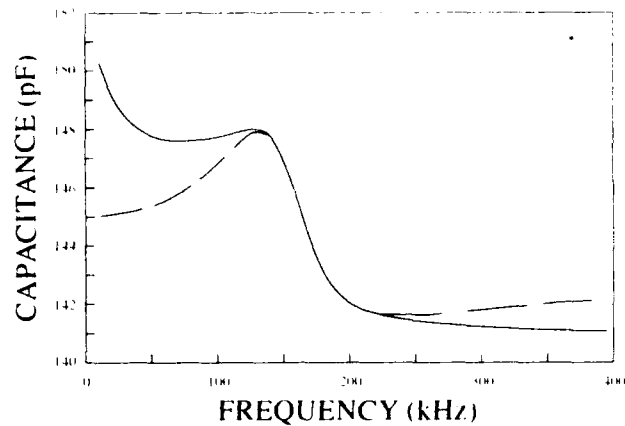


FIG. 7. Measured (solid line) and fitted (dashed) capacitance vs frequency of an NTK 306 sample near the fundamental thickness mode resonance. The fitted line is determined from the measured fundamental thickness mode parameters measured using the technique described in Ref. 1. This demonstrates the need to fit data over limited ranges of frequency.

scribe all of the observed phenomena. The magnitude of this contribution depends on the degree of inaccuracy; and as is usually the case, the assumptions of the model are not well satisfied in the region of a singularity point. Therefore, the model used in these calculations is not accurate at temperatures where the glass transition is observed for a given range of frequency. While the real part of k_t^2 appears to behave in a fairly normal manner, the loss tangent exhibits a rather broad maximum. There appears to be anomalously large values of $\tan \delta_{k_t^2}$ near 0 °C. However, the increased damping of the material at high temperature combined with an asymptotic increase in capacitance due to a low-frequency relaxation prevents precise simultaneous fitting of the capacitance and conductance data impossible over a wide range of frequencies (Fig. 7). This is particularly true for the loss tangent of the electromechanical coupling factor. The poor fit artificially increases the loss tangent of k_t^2 above -20 °C. The high sensitivity of the parameter $\tan \delta_{k_t^2}$ to small changes in the other five parameters is shown in the correlations presented in Table I. This table gives the percentage in the parameter in each column caused by changing the value of the parameter in the row by 1%. Therefore, it gives a sense of the errors involved in the fitting of the data. Elastic and dielectric data seem to behave in an expected manner as does the real part of k_t^2 . For the thickness drive, the observed glass transition region is from -20 °C to +20 °C. For this range of temperatures, the conductance data are weighted more heavily than the capacitance data because they behave in the assumed manner.

2. Thickness extensional drive parameters for NTK 305: Results for the measurements of the fundamental thickness-mode parameters for NTK 305 were similar in form to those measured for NTK 306, but there were significant differences in the magnitudes of many of the electromechanical properties. The series resonance frequency f_s^{TE} , is plotted as a function of temperature in Fig. 8. The resonance frequencies of a 3.8-cm-diam disk are somewhat higher for NTK 305 since the material was thinner (0.228 cm) and is slightly

TABLE I. Interrelationships between parameters obtained by the curve fitting algorithm. Change (in percent) in row parameter for a 1% change in column parameter after iterative calculation is completed.

	k_1^2	$\tan \delta_k^2$	c_{33}^D	$\tan^D \delta_m$	c_{33}^S	$\tan^S \delta_e$
k_1^2	+1	0.6	0.02	+0.0	0.02	+0.04
$\tan \delta_k^2$	0.2	+1	0.12	+0.10	0.01	0.2
c_{33}^D	0.8	2.4	+1	0.9	0.01	0.2
$\tan^D \delta_m$	+0.4	+0.1	0.02	+1	+0.01	+0.04
c_{33}^S	10	8	1	2	+1	+1
$\tan^S \delta_e$	+2	25	0.5	+4.6	+0.01	+1

more compliant as indicated by the elastic stiffness c_{33}^D . The density is 5300 kg/m^3 . The stiffness constant and mechanical loss tangent $\tan^D \delta_m$, are plotted as a function of temperature in Fig. 9. The relaxation in the elastic modulus appears at approximately 10°C . The material has a lower c_{33}^D constant, but above the temperature region where the glass transition is observed, the mechanical loss is several times as high as that of NTK 306 at these frequencies. The clamped dielectric constant ($\epsilon_{33}^l/\epsilon_0$) and electrical loss tangent $\tan^S \delta_e$ are plotted in Fig. 10. The transition appears at a temperature of about -5°C at a frequency of 330 kHz. The electromechanical coupling coefficient squared k_1^2 and associated loss tangent $\tan \delta_k^2$ are plotted as functions of temperature in Fig. 11. Both k_1^2 and $\tan \delta_k^2$ are similar in their temperature dependence, but not in magnitude, to the coupling parameters of NTK 306. The magnitude of the coupling factor of NTK 305 is about twice that of NTK 306. This is most likely due to the larger particle size. It permits superior poling because the ferroelectric domains are free to move.

3. Transverse length thickness (LT 3-1) drive parameters for NTK 306: The third harmonic of the series fundamental transverse length thickness mode (3-1 mode) resonance frequency of a thin bar (dimensions: $3.3 \times 0.40 \times 0.32 \text{ cm}^3$ at 25°C), poled in the thickness direction perpendicular to its length, is plotted as a function of temperature in Fig. 12. For low coupling factor, it is approximately related to the elastic compliance s_{11}^E by

$$f_{3,2}^{LT} \approx (36l^2 \rho s_{11}^E)^{-1/2}, \quad (28)$$

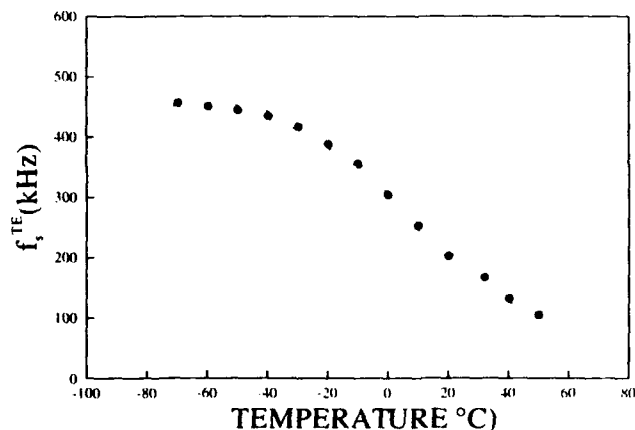


FIG. 8. The series resonance frequency of the fundamental thickness mode of a disk of NTK 305 as a function of temperature.

where l is the length of the thin bar (3.3 cm, the width = 0.20 cm at room temperature). The elastic compliance s_{11}^l and mechanical loss tangent associated with it, are calculated from the impedance data at resonance and plotted in Fig. 13. For this mode, the dielectric constant is measured perpendicular to the mode displacement and the resonance frequency of the LT 3-1 mode is well below the thickness resonance. Consequently, the material is free of stress in the polar direction and the appropriate dielectric parameters, ϵ_{33}^l and $\tan^l \delta_e$, are calculated from the measured capacitance and conductance which are measured directly by the impedance bridge at the series resonance frequency f_s . The third harmonic of the fundamental resonance frequency was fitted rather than the fundamental because of interference from a dielectric relaxation at low frequency. The values of $\epsilon_{33}^l/\epsilon_0$ and $\tan^l \delta_e$ are plotted as a function of temperature in Fig. 14. The effect of the glass transition also causes a relaxation in the dielectric stiffness, or an equivalent increase in the dielectric constant as the temperature is increased. (Dielectric stiffness is the reciprocal of the dielectric permittivity.) The transverse electromechanical coupling factor squared k_{31}^2 of NTK 306 is plotted as a function of temperature in Fig. 15 along with the calculated loss tangent $\tan \delta_{k_{31}}^2$. The transverse coupling factor is very small (less than 1%) and too highly damped at higher temperatures to be accurately analyzed. Some estimate of the parameter can be made at lower temperatures. The loss tangent is undoubtedly inaccurate.

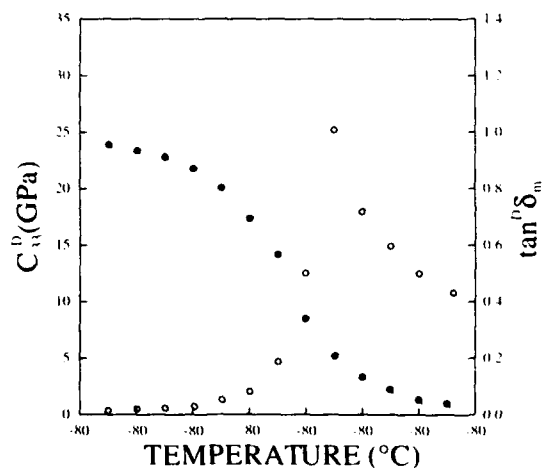


FIG. 9. Elastic stiffness, c_{33}^D (closed symbols), and mechanical loss tangent $\tan^D \delta_m$ (open symbols), of NTK 305 as a function of temperature.

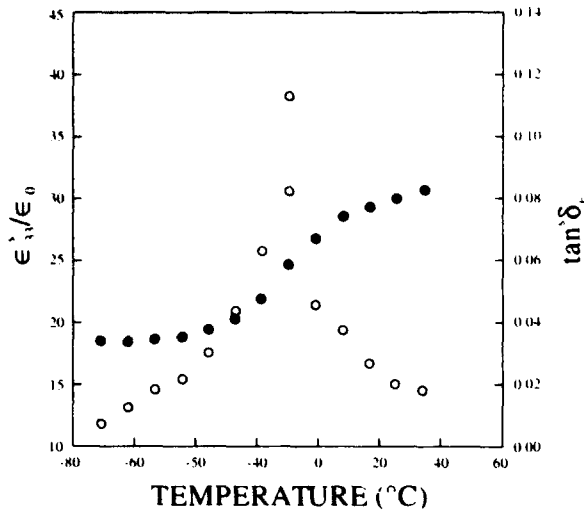


FIG. 10. Clamped dielectric constant, $(\epsilon'_{33}/\epsilon_0)$ (closed symbols), and dielectric loss tangent $\tan \delta_\epsilon$ (open symbols), of NTK 305 as a function of temperature.

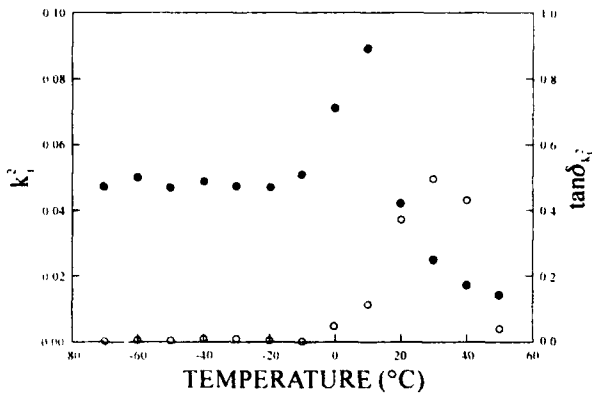


FIG. 11. The square of the electromechanical coupling factor (closed symbols) for the thickness drive k_{31}^2 and the associated loss tangent $\tan \delta_{k_{31}}$ (open symbols), of NTK 305 as a function of temperature.

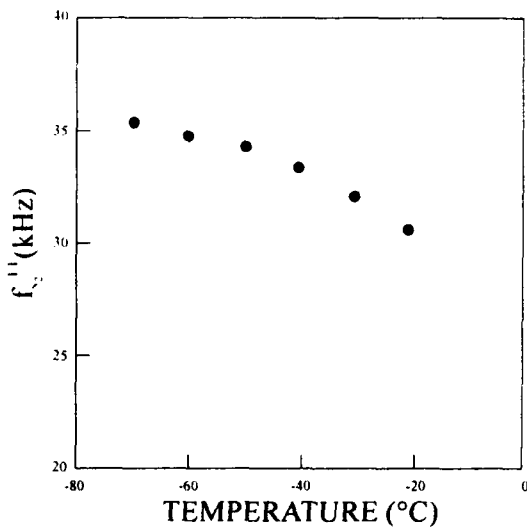


FIG. 12. Transverse length thickness third harmonic (LT 3-1 mode) resonance frequency, f_{31}^{LT} , as a function of temperature of a thin bar of NTK 306 electrically poled in the thickness direction.

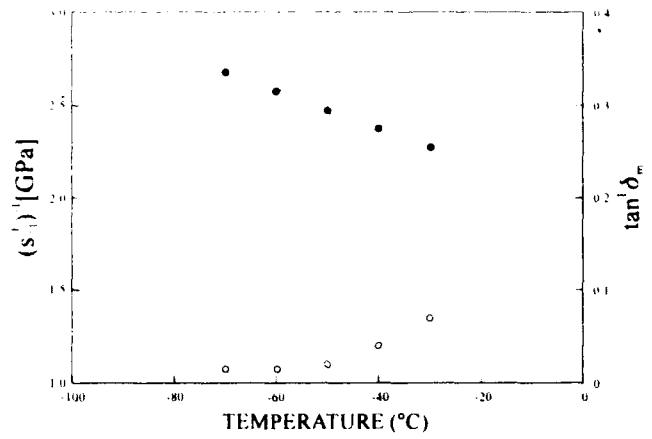


FIG. 13. Reciprocal elastic compliance, $(s'_{11})^{-1}$ (closed symbols), and mechanical loss tangent, $\tan \delta_m$ (open symbols), of NTK 306 as a function of temperature.

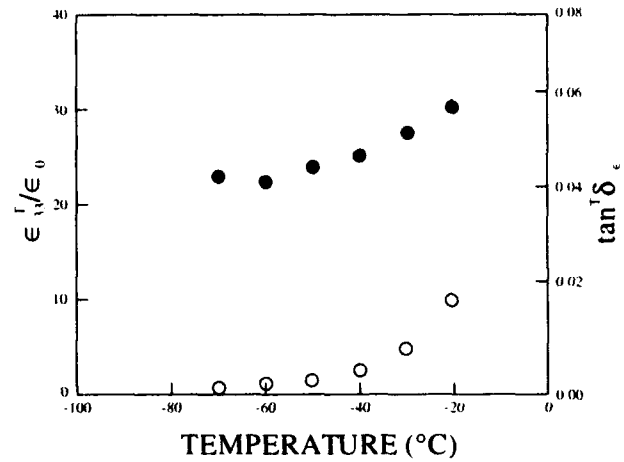


FIG. 14. Free dielectric constant, $(\epsilon'_{33}/\epsilon_0)$ (closed symbols), and dielectric loss tangent, $\tan \delta_\epsilon$ (open symbols), of NTK 306 as a function of temperature.

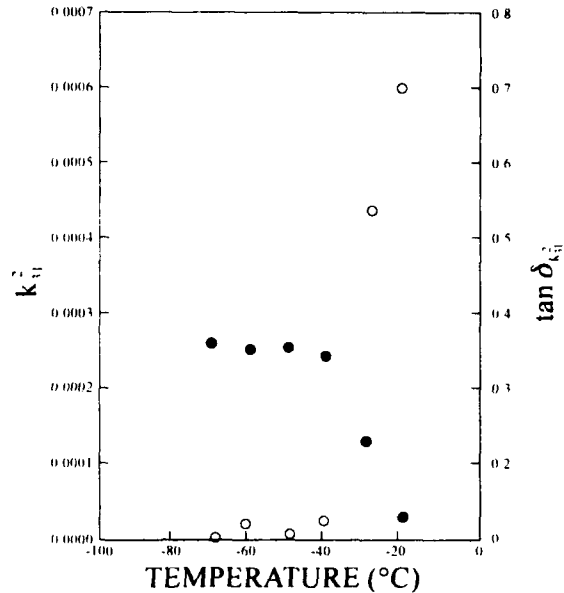


FIG. 15. Square of the transverse electromechanical coupling coefficient, k_{31}^2 (closed symbols), and associated loss tangent, $\tan \delta_{k_{31}}$ (open symbols), of NTK 306 plotted as a function of temperature.

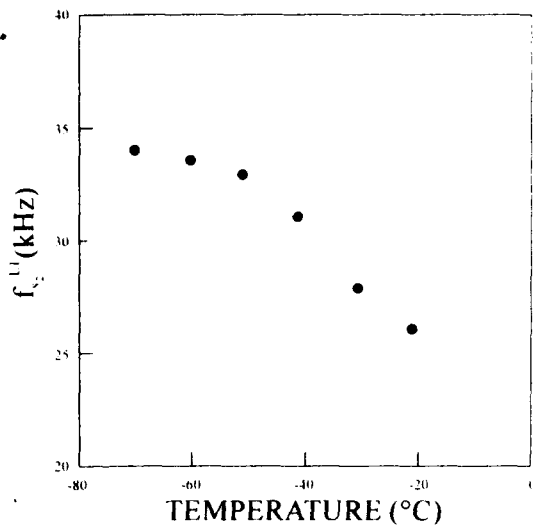


FIG. 16. Series resonance frequency $f_{31}^{(1)}$, of the third harmonic transverse length thickness LT mode of a thin bar of NTK 305 as a function of temperature from -70°C to -20°C .

particularly near the transition region, for reasons discussed before.

4. Transverse length thickness drive parameters for NTK 305: The transverse length-thickness (LT) resonance frequency (third harmonic of the fundamental) of a thin bar (dimensions: $3.3 \times 0.40 \times 0.23 \text{ cm}^3$ at 25°C) of NTK 305 is plotted in Fig. 16 as a function of temperature from -70°C to -20°C . The elastic compliance s_{11}^E ; free dielectric constant, $(\epsilon_{33}^T/\epsilon_0)$; electromechanical coupling factor-squared k_{31}^2 ; and the associated loss tangents are plotted in Figs. 17–19, respectively. The lateral coupling factor k_{31} of NTK 305 is larger than that of NTK 306 but is still very small compared with the thickness coupling factor. The dielectric constant is also larger due to the larger particle size of NTK 305. This clamps the piezoelectric effect less effectively. The effect of the glass transition on the observed properties is not fully apparent because of the limited temperature range of the measurements; but the slope of the curves, particularly of

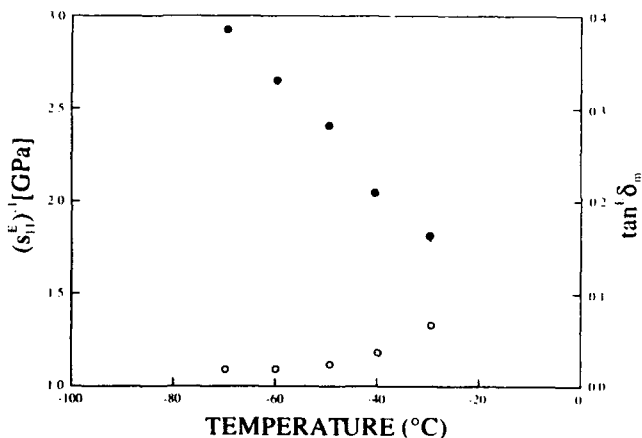


FIG. 17. Reciprocal elastic compliance, $(s_{11}^E)^{-1}$ (closed symbols), and mechanical loss tangent, $\tan^E \delta_m$ (open symbols), of NTK 305 as a function of temperature.

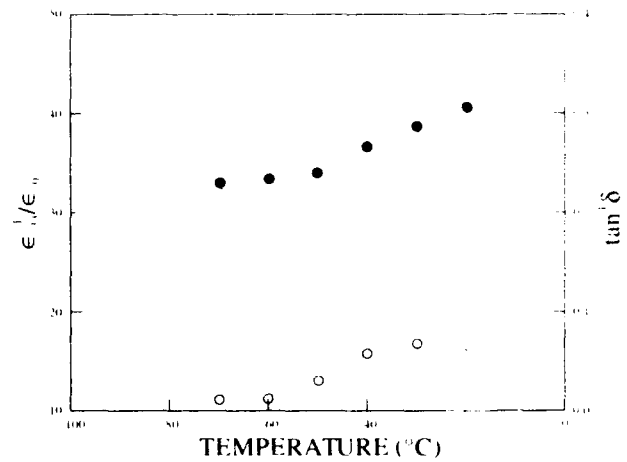


FIG. 18. Free dielectric constant, $(\epsilon_{33}^T/\epsilon_0)$ (closed symbols), and dielectric loss tangent $\tan^E \delta_e$ (open symbols), of NTK 305 as a function of temperature.

the elastic constant and mechanical loss tangent, shows that the effect of the transition is imminent.

C. Determination of the shift function from dielectric and elastic constant measurements

The real and imaginary parts of the dielectric constants were measured over a frequency range of 1 to 200 kHz. The procedure for determining the shift factor for determining elastic properties over wide ranges of temperature and frequency is described in detail by Ferry.² It essentially involves shifting measurements of both real and imaginary parts of the elastic or dielectric properties made at different temperatures over a set range of frequency below the thickness resonance such that they fit together in a smooth Debye-like curve. The piezoelectric resonance peaks are very narrow compared with the broad relaxation spectrum of the polymer.

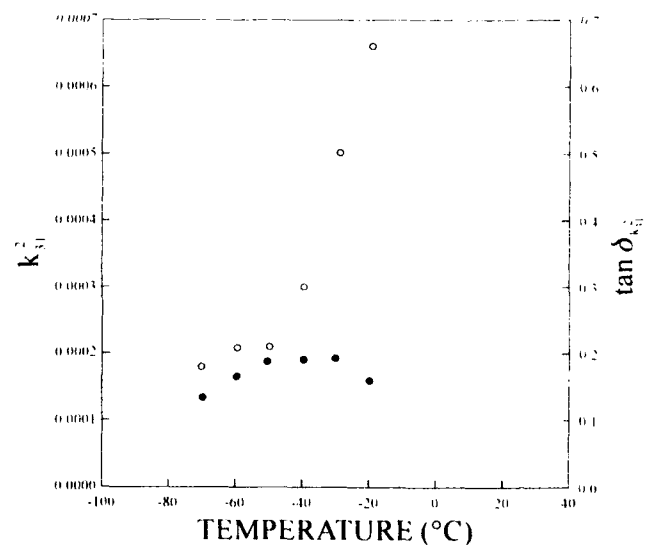


FIG. 19. Square of the transverse electromechanical coupling coefficient, k_{31}^2 (closed symbols), and associated loss tangent, $\tan \delta_{k_{31}}$ (open symbols), of NTK 305 plotted as a function of temperature.

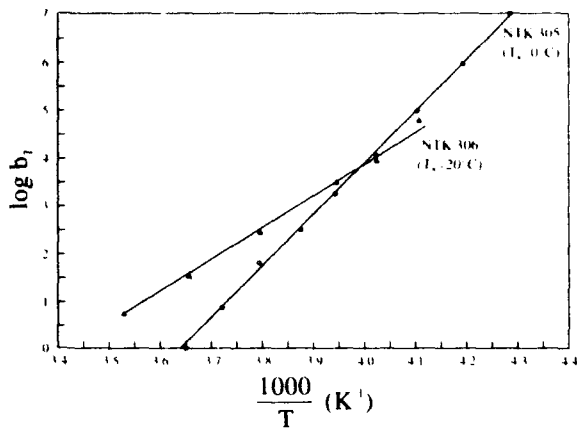


FIG. 20. Dielectric shift factor b_T as a function of reciprocal temperature for NTK 305 and NTK 306.

They are superimposed on the dielectric relaxation spectra. The locations of the resonance peaks relative to the dielectric relaxation peak change as the temperature is varied. The height of the resonance peaks decreases in the vicinity of the glass transition region where the mechanical loss is large. Shifting is done primarily with respect to frequency, but small vertical shifts are required to account for experimental error and thermal expansion. These are insignificant in this case. For the dielectric data, the Arrhenius-type shift in Eq. (12) was found to fit the experimental data quite well over the temperature range from -30°C to $+20^\circ\text{C}$, thereby covering the glass-transition region of the polymer where the electromechanical properties are changing significantly. For NTK 306, the least-squares fit of $\log b_T$ versus T^{-1} was linear with a correlation coefficient of 0.998 (Fig. 20). The value of the shift constant, b_T/k , in Eq. (12) was determined to be 7400°K Eq. (13). Thus, near 0°C ($T_r=273^\circ\text{K}$), a decrease in temperature of 10° will change the dielectric properties by the same amount as a decade increase in frequency. For instance,

$$\log \frac{\omega}{\omega_0} = 7400^\circ\text{K} \left(\frac{1}{263^\circ\text{K}} - \frac{1}{273^\circ\text{K}} \right), \quad (29)$$

is close to unity indicating a shift of one decade for a 10° shift in temperature. The value of A_T/k determined from measurements of s_{11}^E using the vibration resonance technique was 9400 .¹⁰ The magnitude of the elastic shift parameter of NTK 306 is 1.5 times that determined from dielectric data as well as that observed for carbon-filled polychloroprene rubber.⁸ The free dielectric constant is only mildly affected by the glass transition because of the very small lateral coupling factor k_{31} (approximately 1%) of NTK 305.

For NTK 305, the Arrhenius-type relationship in Eq. (11) was also found to fit the experimental data extremely well with a correlation coefficient of 0.999 for the plot of $\log b_T$ vs T^{-1} (Fig. 20). The constant A_T/k was calculated to be $10\,300$ ($T_r=293^\circ\text{K}$), which is even larger than the value for NTK 306. This value is virtually identical to the value ($10\,380$) determined from elastic constant measurements.

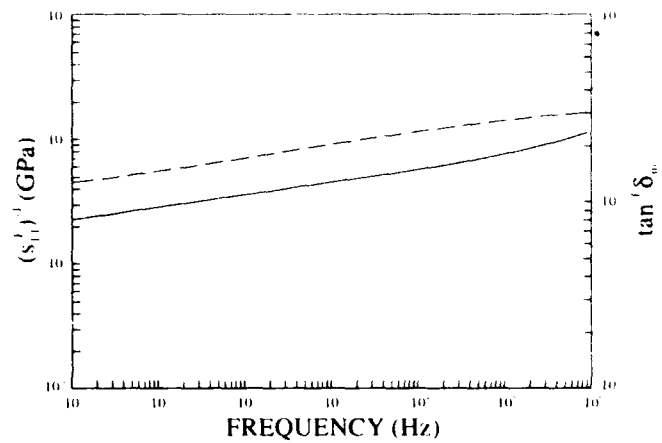


FIG. 21. Reciprocal elastic compliance, $(s_{11}^E)^{-1}$ (solid line), and mechanical loss tangent, $\tan^E \delta_m$ (dashed line), of NTK 306 measured using vibrational resonance technique as a function of frequency referred to a temperature of 0°C .

D. Independent elastic property measurements

The values of $(s_{11}^E)^{-1}$ obtained from the vibrational resonance technique were determined for both NTK 305 and NTK 306. The time-temperature shift was applied in both cases, and the data were seen to follow the Arrhenius-type of shift factor. This shift factor was used² to produce the isothermal measurement of s_{11}^E vs frequency and loss tangent shown in Fig. 21 for NTK 306 and for NTK 305 in Fig. 22. The data are shifted to a reference temperature of 0°C .

E. Estimation of Poisson's ratio

The approximate values of Poisson's ratio, as estimated from Eqs. (24) and (25) using the frequency shifted measurements of c_{33}^D and s_{11}^E , are plotted in Figs. 23 and 24 for NTK 306 and NTK 305, respectively, as functions of temperature. The frequency shift was calculated using Eq. (12). The value of s_{11} was measured at 31 kHz. In the case of NTK 306, the glass transition causes the value of ν to increase from about

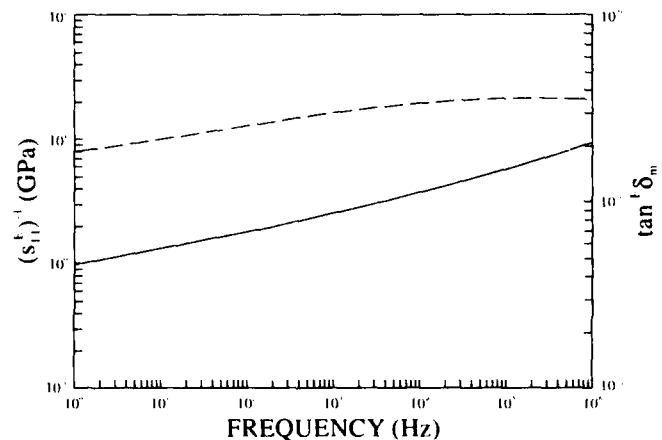


FIG. 22. Reciprocal elastic compliance, $(s_{11}^E)^{-1}$ (solid line), and mechanical loss tangent, $\tan^E \delta_m$ (dashed line), of NTK 305 measured using vibrational resonance technique as a function of frequency referred to a temperature of 0°C .

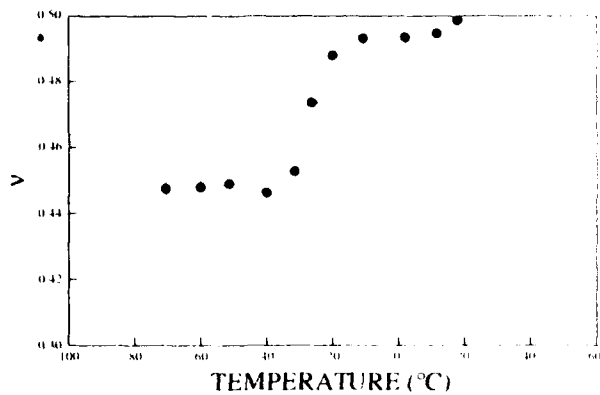


FIG. 23. Poisson's ratio ν for NTK 306 at frequency of 1 Hz as calculated from measurements of c_{33}^D and s_{11}^E as a function of temperature.

0.45 to 0.495. The value of ν should, of course, approach 0.5 in the rubbery region above T_g if the material is newly isotropic. For NTK 305, there is no obvious increase in ν at the glass transition as observed in NTK 306. The value of Poisson's ratio remains fairly constant at around 0.47 and does not vary outside the error of the measurement. It perhaps shows a slight increase, as expected; but this is not clear because of the scatter in the calculated result. Both results indicate that the material behaves elastically like a filled isotropic rubber.

IV. DISCUSSION

A. Influence on hydrostatic piezoelectric coefficients

The glass transition strongly influences the elastic, dielectric, and piezoelectric properties of piezoelectric composite materials including both NTK 305 and NTK 306. This is demonstrated by relaxation phenomena in the real parts of the elastic constants, the dielectric permittivity, the square of the electromechanical coupling coefficients, and by maxima in the loss tangents associated with some of these properties. The transition in the real and imaginary parts of the free dielectric constant appears incipient, but it is not clearly visible due to the low electromechanical coupling and high damping of the transverse mode.

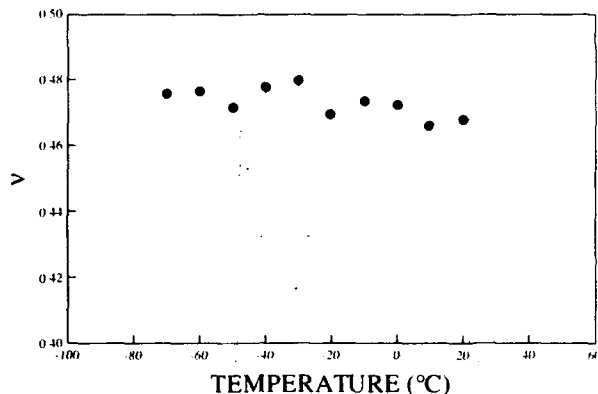


FIG. 24. Poisson's ratio ν for NTK 305 at 1 Hz calculated from measurements of c_{33}^D and s_{11}^E as a function of temperature.

The model used to estimate the electromechanical coupling parameters fits experimental data successfully over a temperature range from -70°C to 20°C . Above 20°C , the conductance data can be fitted well in the vicinity of the fundamental thickness resonance. However, due to a low-frequency relaxation, the model can be accurately fitted to the capacitance data only above the series resonance frequency. In the middle of the observed transition (-10°C to $+10^\circ\text{C}$), both capacitance and conductance data marginally fit the model. However, even in this region, the computed values for the real and imaginary parts of the elastic and dielectric constants are reasonable.

For temperatures where the lateral mode is measurable, the magnitude of the ratio of the thickness coupling coefficient k_t to transverse coupling coefficient k_{31} , is on the order of 20 for both NTK 305 and NTK 306. This difference indicates that the lateral piezoelectric constant d_{31} is much smaller than d_{33} and the material should have a significant hydrostatic piezoelectric constant d_h , since

$$d_h = d_{33} + 2d_{31}, \quad (30)$$

although d_{33} and d_{31} are opposite in sign. This effect has been observed by experiment using an acoustic reciprocity technique¹¹ where d_h was measured to be 40×10^{-12} m/V for NTK 305 and 20×10^{-12} m/V for NTK 306 at 25°C ¹² while d_{33} was measured to be 46×10^{-12} for NTK 305 and 34×10^{-12} m/V for NTK 306 also at 25°C . Thus d_{31} is less than 20% of d_{33} for NTK 306 and less than 3% of d_{33} for NTK 305, which is in good agreement with the results of the resonance measurement.

B. Application of the time-temperature superposition principle

The temperature dependence of the dielectric and mechanical properties of both NTK 306 and NTK 305 is described by the Arrhenius-type equation. The constant, E^*/k , in Eq. (12) was the same for NTK 305 regardless of whether it was determined from dielectric or elastic properties. For NTK 306, the shift factor measured electrically was about two-thirds of that measured acoustically. By comparison, the glass-transition temperature as measured by DSC is approximately -35°C . By equating the thermal strain rate, or time derivative (denoted by the superposed dot) of the volume thermal volume expansion rate produced in the DSC experiment with the volume strain rate produced in the sample by the measuring electric field E in the resonance experiment,

$$\Delta \dot{V}/V = \alpha_p \Delta \dot{T} = d_h \dot{E}, \quad (31)$$

where α_p is the volume thermal expansion coefficient, an estimate can be made of the frequency in the resonance experiment which produces a strain rate equivalent to that in the DSC measurement. Assuming a harmonic field of the form,

$$E = E_0 e^{i2\pi ft}, \quad (32)$$

and substituting it into Eq. (32) along with the known values of E_0 (500 V/m), heating rate (0.67 $^\circ\text{C}/\text{s}$), and piezoelectric d_h coefficient (20×10^{-12} m/V for NTK 306), and thermal expansion (1.5×10^{-4} $^\circ\text{K}$), one would expect the DSC mea-

surement to correspond to a resonance measurement made near a frequency of 1000 Hz. This frequency is approximately 2.4 decades lower than f_v^{TE} . Since the apparent glass-transition temperature of rubber materials shifts about 10 °C for each decade of frequency (reference temperature equals 0 °C), one would expect the transition in the TE mode should occur at -11 °C. The actual data shown in Figs. 3 and 4 concur with these predictions.

The dielectric relaxation associated with interfacial polarization dominates the dielectric spectra at frequencies below approximately 1 kHz. This effect is present in all multiphase materials where the dielectric permittivities and electrical conductivities of the various phases differ. It occurs at electrode-dielectric interfaces. In many cases, the effects occur at such a sufficiently low frequency that they often are not significant. However, in the NTK composite materials, these effects are important and limit the range of frequency over which the time-temperature superposition principle can be applied to dielectric data. However, the technique is still extremely useful for extrapolating high-frequency dielectric measurements to frequencies used in underwater acoustic applications. Of course, the technique is often used in extending elastic property measurements over wider ranges of frequency.

While the time-temperature superposition principle was applied successfully to the dielectric data used in these measurements, it is not necessarily valid for extrapolating piezoelectric measurements. Computing these parameters using the frequency-temperature relationship at frequencies away from resonance using the same data is perhaps possible, but is not attempted here. One would have to measure these shift factors independently. For NTK 305, the dielectric and elastic shift functions are identical and one might extrapolate the measurements to piezoelectric coefficients as well. Such a procedure would be straightforward if the piezoelectric e_{31} and e_{33} coefficients, which relate dielectric displacement to strain in the material, was independent of frequency. However, direct measurements of this parameter in several piezoelectric materials indicate that it exhibits relaxational behavior as well.^{13,14}

Further work could focus on measuring the piezoelectric properties of these materials independently as a function of temperature and determining their time-temperature shift

constants if possible. These measurements are more difficult but would provide an important verification of the measurements described here. Measurements of different-sized samples of these materials using the resonance method would also provide an alternate but less complete method of measuring the frequency dependence of the electromechanical properties at constant temperature. Such information could be used in conjunction with the time-temperature superposition principle and possibly allow for extensive property measurements over the relevant portion of the temperature-frequency plane.

ACKNOWLEDGMENTS

The author wishes to thank Dr. Rodger Capps, Dr. Joseph Zalesak, Dr. Robert Montgomery, and Craig Brown for their helpful comments in preparing this manuscript. This work was supported by the Office of Naval Research.

- ¹Q. C. Xu, A. R. Ramachandran, and R. E. Newnham, "Resonance measuring technique for complex coefficients of piezoelectric composites," *J. Wave Mater. Inter.* **2**, 105-18 (1987).
- ²J. D. Ferry, *Viscoelastic Properties of Polymers* (Wiley, New York, 1970), 2nd ed.
- ³R. T. Bailey, A. M. North, and R. A. Pethrick, *Molecular Motion in High Polymers* (Clarendon, Oxford, 1981).
- ⁴P. Hedvig, *Dielectric Spectroscopy of Polymers* (Halsted, New York, 1977).
- ⁵F. Rodriguez, *Principles of Polymer Systems* (McGraw-Hill, New York, 1970).
- ⁶J. F. Nye, *Physical Properties of Crystals and Their Representation by Tensors and Matrices* (Clarendon, Oxford, 1957).
- ⁷K. C. Rusch and R. H. Beck, Jr., "Yielding behavior of glassy polymers. III. Relative influence of free volume and kinetic energy," *J. Macromol. Sci. B* **4**, 621 (1970).
- ⁸R. N. Capps, "Influence of carbon black fillers on the acoustic properties of polychloroprene (neoprene) rubbers," *J. Acoust. Soc. Am.* **78**, 406 (1985).
- ⁹R. N. Capps, "Dynamic Young's moduli of some commercially available polyurethanes," *J. Acoust. Soc. Am.* **73**, 2000 (1983).
- ¹⁰R. N. Capps (private communication).
- ¹¹R. S. Bobber, *Underwater Electroacoustic Measurements* (U.S. Government Printing Office, Washington, DC), pp. 38-41.
- ¹²K. M. Rittenmyer (unpublished).
- ¹³T. Furukawa, J. Aiba, and E. Fukada, "Piezoelectric relaxation in polyvinylidene fluoride," *J. Appl. Phys.* **50**, 3615 (1979).
- ¹⁴K. Hamano and T. Yamaguchi, "Piezoelectric relaxation in ferroelectrics and polymers," *Ferroelectrics* **42**, 23 (1982).
- ¹⁵K. M. Rittenmyer, Proceedings of the 1990 International Symposium on the Applications of Ferroelectrics held in Urbana, IL, in June 1990.

Accession For		
NTIS	CRA&I	<input checked="" type="checkbox"/>
DTIC	TAB	<input type="checkbox"/>
Unannounced		<input type="checkbox"/>
Justification		
By		
Distribution /		
Availability Codes		
Dist	Avail and/or Special	
A-1	20	